Cu-Ag

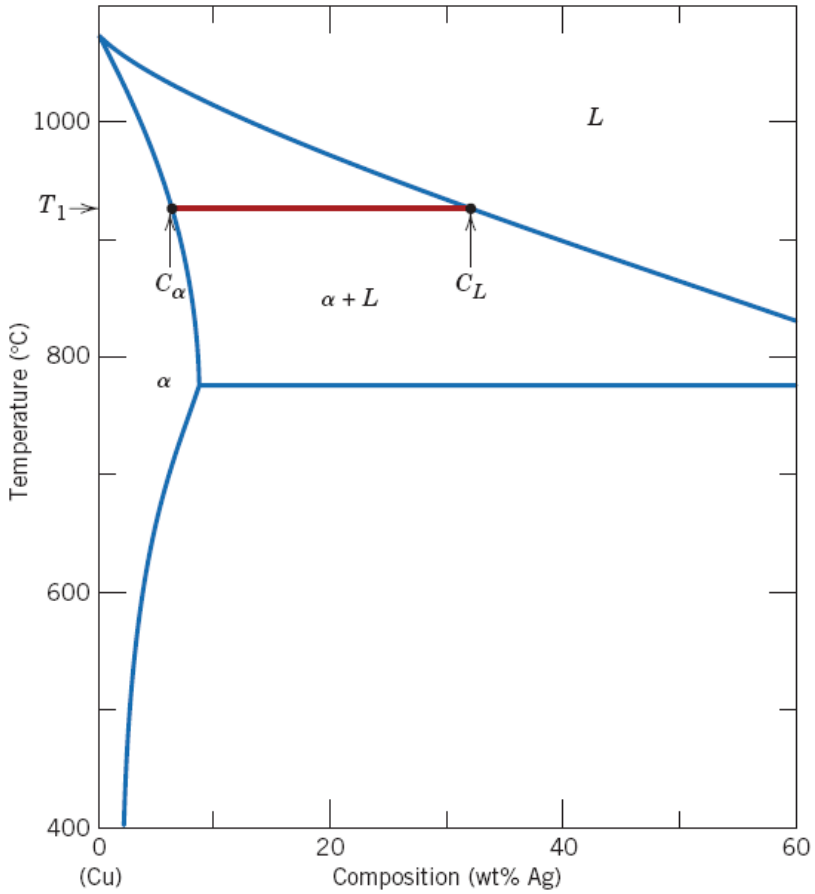

Figure 9.23 Enlarged copper-rich section of the Cu–Ag phase diagram in which the Gibbs phase rule for the coexistence of two phases (α and L) is demonstrated. Once the composition of either phase (C_α or C_L) or the temperature (T_1) is specified, values for the two remaining parameters are established by construction of the appropriate tie line.

Pb-Sn

Figure 9.13 Schematic representations of the equilibrium microstructures for a lead–tin alloy of eutectic composition C_3 above and below the eutectic temperature.

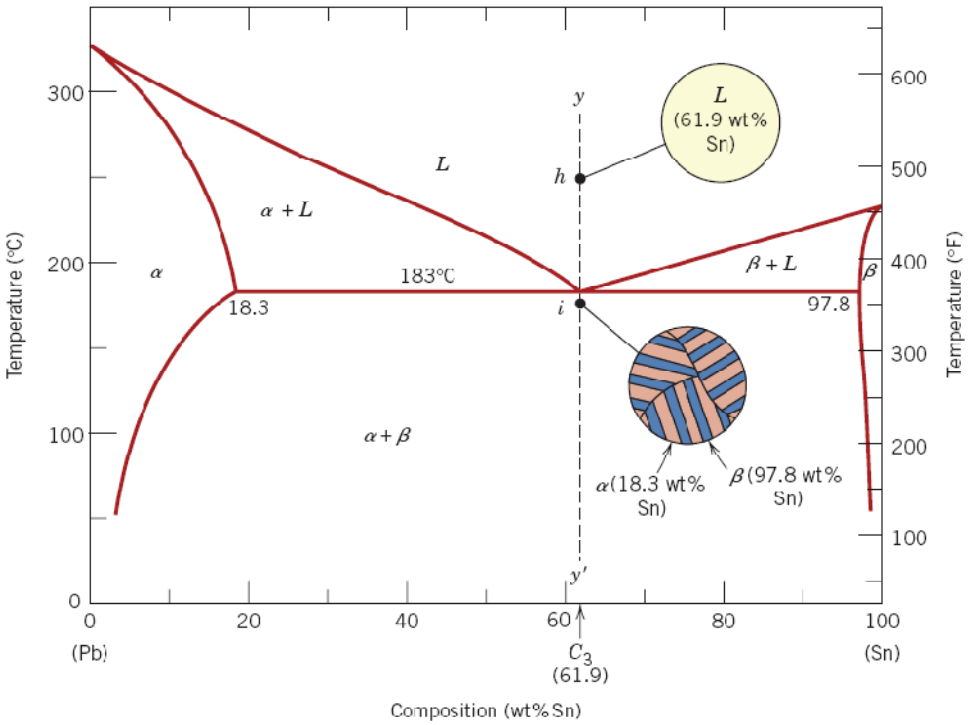

Ni-Ti

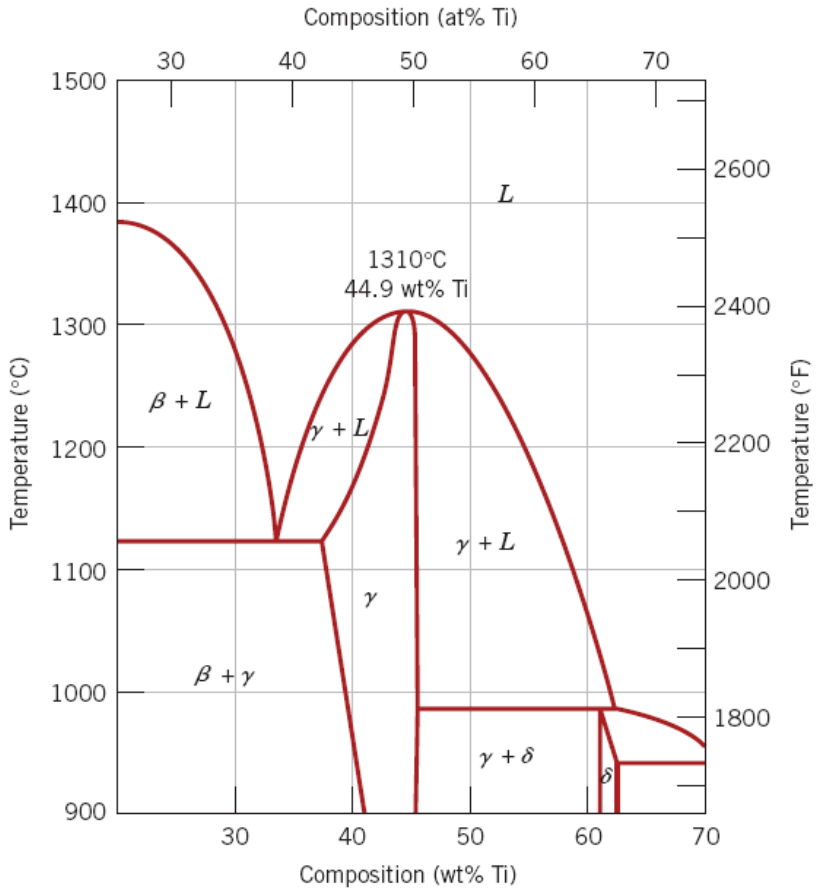

Figure 9.22 A portion of the nickel–titanium phase diagram on which is shown a congruent melting point for the γ-phase solid solution at 1310°C and 44.9 wt% Ti. [Adapted from *Phase Diagrams of Binary Nickel Alloys*, P. Nash (Editor), 1991. Reprinted by permission of ASM International, Materials Park, OH.]

Mg-Pb

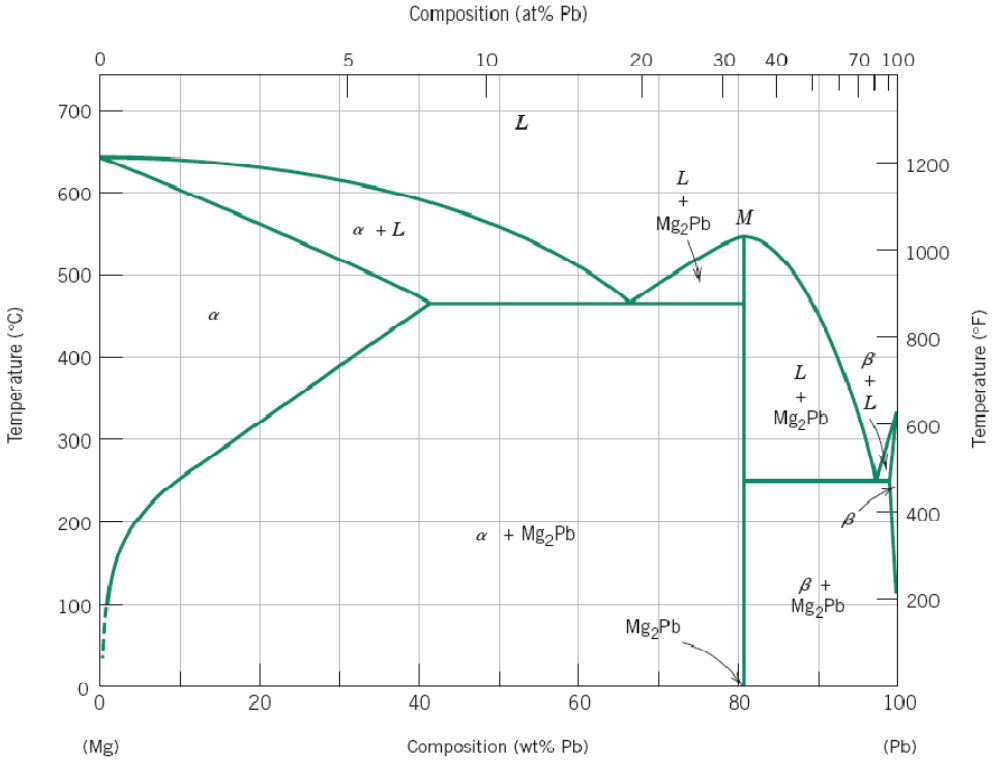

Figure 9.20 The magnesium–lead phase diagram. [Adapted from *Phase Diagrams of Binary Magnesium Alloys*, A. A. Nayeb-Hashemi and J. B. Clark (Editors), 1988. Reprinted by permission of ASM International, Materials Park, OH.]

Cu-Zn

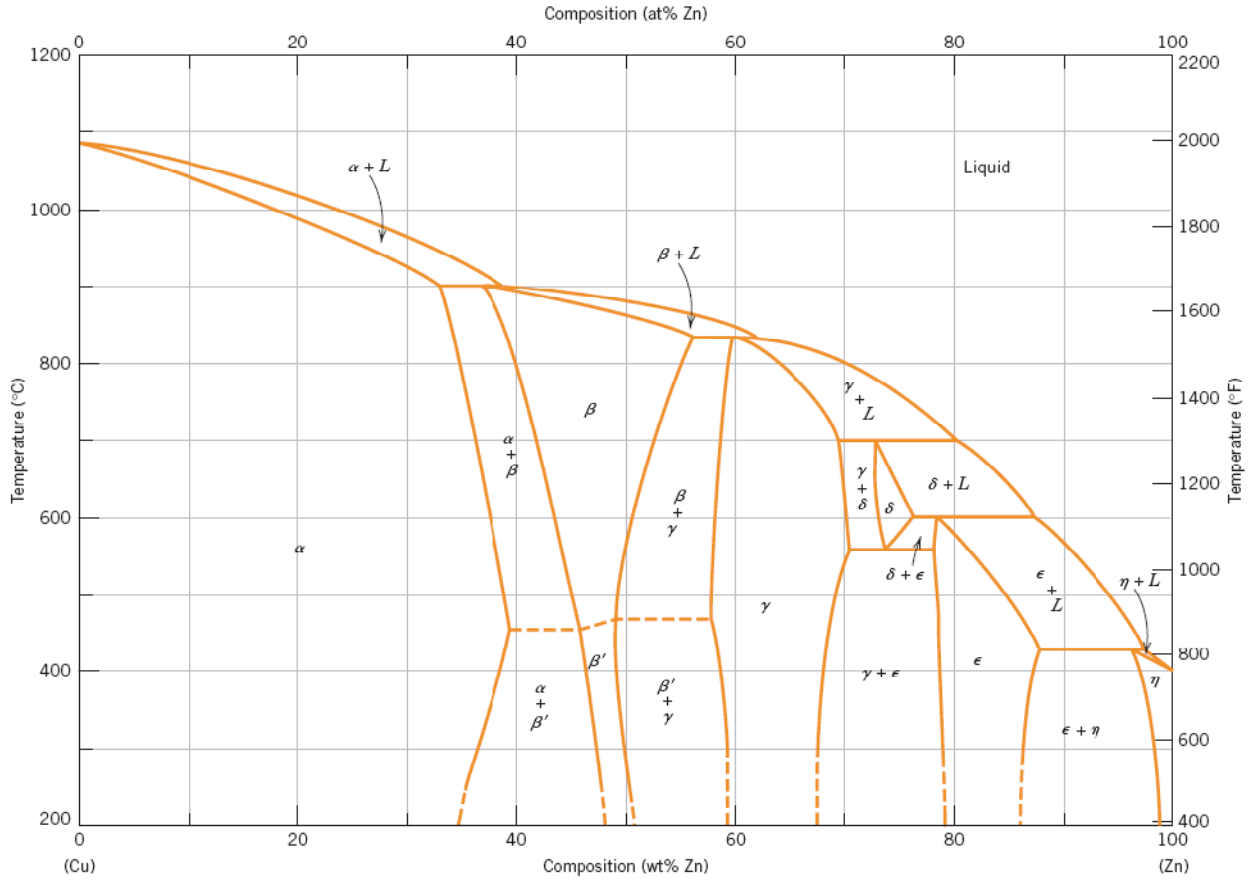

Figure 9.19 The copper–zinc phase diagram. [Adapted from *Binary Alloy Phase Diagrams*, 2nd edition, Vol. 2, T. B. Massalski (Editor-in-Chief), 1990. Reprinted by permission of ASM International, Materials Park, OH.]

Fe-Fe_3C

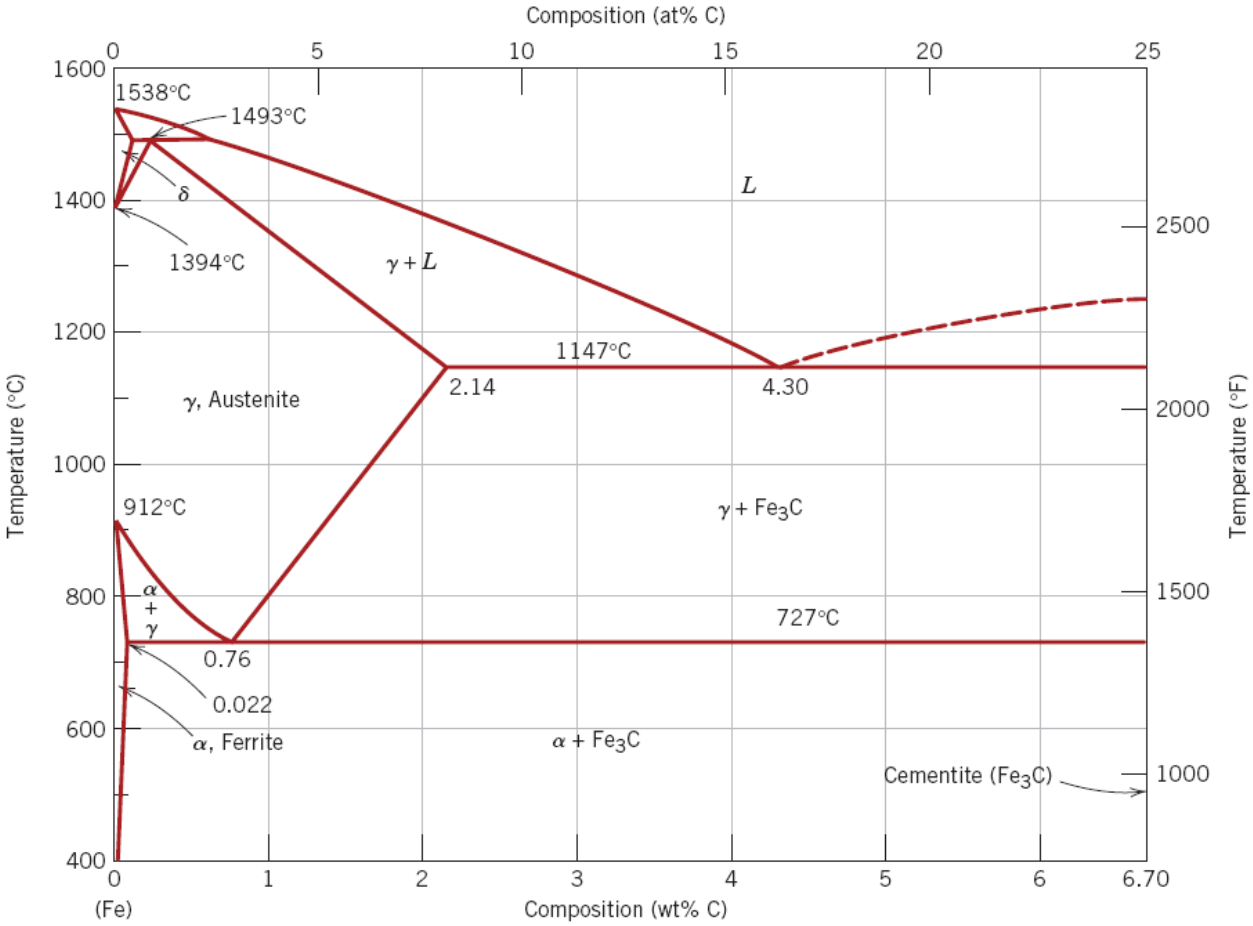

Figure 9.24 The iron–iron carbide phase diagram. [Adapted from *Binary Alloy Phase Diagrams,* 2nd edition, Vol. 1, T. B. Massalski (Editor-in-Chief), 1990. Reprinted by permission of ASM International, Materials Park, OH.]